A 3D cine-MRI acquisition technique and image analysis framework to quantify bowel motion demonstrated in gynecological cancer patients

Danique L.J. Barten[a] and Janna J. Laan
Department of Radiation Oncology, Amsterdam University Medical Centers, University of Amsterdam, Meibergdreef 9, 1105 AZ Amsterdam, The Netherlands

Koen J. Nelissen
Department of Radiation Oncology, Amsterdam University Medical Centers, Vrije Universiteit Amsterdam, De Boelelaan 1117, 1081 HV Amsterdam, The Netherlands

Jorrit Visser, Henrike Westerveld and Arjan Bel
Department of Radiation Oncology, Amsterdam University Medical Centers, University of Amsterdam, Meibergdreef 9, 1105 AZ Amsterdam, The Netherlands

Catharina S. de Jonge and Jaap Stoker
Department of Radiology and Nuclear Medicine, Amsterdam University Medical Centers, University of Amsterdam, Meibergdreef 9, 1105 AZ Amsterdam, The Netherlands

Zdenko van Kesteren
Department of Radiation Oncology, Amsterdam University Medical Centers, University of Amsterdam, Meibergdreef 9, 1105 AZ Amsterdam, The Netherlands

(Received 25 November 2020; revised 1 February 2021; accepted for publication 5 March 2021; published 7 April 2021)

Purpose: Magnetic resonance imaging (MRI) is increasingly used in radiation oncology for target delineation and radiotherapy treatment planning, for example, in patients with gynecological cancers. As a consequence of pelvic radiotherapy, a part of the bowel is irradiated, yielding risk of bowel toxicity. Existing dose-effect models predicting bowel toxicity are inconclusive and bowel motion might be an important confounding factor. The exact motion of the bowel and dosimetric effects of its motion are yet uncharted territories in radiotherapy. In diagnostic radiology methods on the acquisition of dynamic MRI sequences were developed for bowel motility visualization and quantification. Our study aim was to develop an imaging technique based on three-dimensional (3D) cine-MRI to visualize and quantify bowel motion and demonstrate it in a cohort of gynecological cancer patients.
Methods: We developed an MRI acquisition suitable for 3D bowel motion quantification, namely a balanced turbo field echo sequence (TE = 1.39 ms, TR = 2.8 ms), acquiring images in 3.7 s (dynamic) with a $1.25 \times 1.25 \times 2.5$ mm^3 resolution, yielding a field of view of $200 \times 200 \times 125$ mm^3. These MRI bowel motion sequences were acquired in 22 gynecological patients. During a 10-min scan, 160 dynamics were acquired. Subsequent dynamics were deformably registered using a B-spline transformation model, resulting in 159 3D deformation vector fields (DVFs) per MRI set. From the 159 DVFs, the average vector length was calculated per voxel to generate bowel motion maps. Quality assurance was performed on all 159 DVFs per MRI, using the Jacobian Determinant and the Harmonic Energy as deformable image registration error metrics. In order to quantify bowel motion, we introduced the concept of cumulative motion–volume histogram (MVH) of the bowel bag volume. Finally, interpatient variation of bowel motion was analyzed using the MVH parameters M10%, M50%, and M90%. The M10%/M50%/M90% represents the minimum bowel motion per frame of 10%/50%/90% of the bowel bag volume.
Results: The motion maps resulted in a visualization of areas with small and large movements within the bowel bag. After applying quality assurance, the M10%, M50%, and M90% were 4.4 (range 2.2–7.6) mm, 2.2 (range 0.9–4.1) mm, and 0.5 (range 0.2–1.4) mm per frame, on average over all patients, respectively.
Conclusion: We have developed a method to visualize and quantify 3D bowel motion with the use of bowel motion specific MRI sequences in 22 gynecological cancer patients. This 3D cine-MRI-based quantification tool and the concept of MVHs can be used in further studies to determine the effect of radiotherapy on bowel motion and to find the relation with dose effects to the small bowel. In addition, the developed technique can be a very interesting application for bowel motility assessment in diagnostic radiology. © *2021 The Authors. Medical Physics published by Wiley Periodicals LLC on behalf of American Association of Physicists in Medicine.* [https://doi.org/10.1002/mp.14851]

Key words: 3D cine-MRI, bowel motion quantification, bowel motion visualization, deformable image registration, motion–volume histogram

1. INTRODUCTION

The use of magnetic resonance imaging (MRI) as a noninvasive technique to assess or diagnose abdominal diseases has expanded rapidly the past decades. Visualization and quantification of bowel motion, for example, due to gastrointestinal motility and breathing, with MRI is extensively shown to be feasible in diagnostic radiology.[1-6] These methods rely on the acquisition of dynamic MRI sequences that capture bowel movements between multiple time frames. MRI studies on bowel motility have mainly used two-dimensional (2D) techniques and sophisticated motion analysis software for bowel motility visualization and quantification.[7-9]

In the radiotherapy field, MRI is increasingly used before and during treatment for target delineation, treatment planning, and response evaluation, especially in radiotherapy for an abdominal malignancy, such as gynecological cancer. In patients treated with curative radiotherapy for gynecological cancer, part of the bowel region is irradiated. Therefore, the bowel is an important organ at risk (OAR). In this patient group, acute and late gastrointestinal toxicities (GI) are common of which diarrhea and proctitis are the most frequently scored GI symptoms.[10-13] In addition, abdominal surgery is an independent risk factor for severe GI toxicity,[14] presumably due to adhesions that might restrict bowel motion.

In order to reduce the risk of these GI toxicities, studies aiming to identify toxicity-related dose–volume parameters that can be used to define dose constraints for the tumor-surrounding OAR. Subsequently, these constraints can be used to guide treatment planning protocols to limit the risk of toxicity and simultaneously ensure optimal dose delivery to the clinical target volume. All available data regarding dose–volume parameters related to gastrointestinal toxicity were summarized in the Quantitative Analysis of Normal Tissue Effects in the Clinic (QUANTEC) reviews, focusing on rectum and small bowel.[15] Kavanagh et al. suggested that acute and late small bowel toxicity are related to maximum dose and/or volume threshold parameters.[16] However, the authors did not show a detailed dose–volume relationship analysis.

Furthermore, another important aspect that should be considered when evaluating dose–volume parameters of the bowel is that the bowel is a highly mobile organ, which almost certainly introduces uncertainties in dose–volume-related parameters. Jadon et al. systematically reviewed studies examining the dose–volume predictors of all components of the bowel for late toxicity and identified that bowel motion is a confounding factor in determining dose–volume relationships.[17] This finding was in line with two other studies.[18,19] However, the type of bowel motion (e.g., contractions caused by segmentation or peristalsis, or displacement) and the subsequent potential dosimetric effects are yet uncharted territories in the field of radiotherapy.

Given the occurrence and impact of bowel toxicity in gynecological cancer patients and the possible effect of bowel motion on the actual delivered dose, there is a need to take bowel motion into account in radiotherapy treatment planning. For optimal assessment of bowel motion parameters, the MRI acquisition needs to have (a) a large field of view to map motion in the high-radiation dose region, (b) a high enough temporal resolution (i.e., a high sampling rate) to capture movements that take place on a short timescale, and (c) a high enough spatial resolution to measure bowel motion with sufficient accuracy. Altogether, there is an urgent need for a three-dimensional (3D) imaging protocol and software tools for visualization and quantification of the images.

Until now 3D bowel motion has not yet been quantified for radiotherapy purposes. The aim of our study was to develop a technique to visualize, analyze, and quantify bowel motion with high-quality cine-MRI in 3D and demonstrate the applicability in a cohort of gynecological cancer patients.

2. MATERIALS AND METHODS

2.A. Motion assessment: visualization and quantification

For the visualization and quantification of bowel motion, a framework was developed, consisting of a 3D cine-MRI acquisition technique and image analysis software tools. This framework is schematically represented in Fig. 1 and further explained below.

2.A.1. Step 1: Three-dimensional MRI acquisition

With a 3T Philips Ingenia MRI scanner (Philips, Best, Netherlands), a 3D cine-MRI acquisition suitable for 3D bowel motion visualization and quantification was generated. Scans were acquired in supine position using a combination of the posterior coil located in the table and an anterior torso-coil covering the entire abdominal region. After initial survey sequences, a balanced turbo field echo (BTFE) sequence was used with the following parameters: TE/TR: 1.39/2.8 ms; spatial resolution: 1.25 × 1.25 × 2.5 mm^3; field of view of 200 × 200 × 125 mm^3, resulting in a temporal resolution of one image every 3.7 s. The BTFE sequence has a high signal over noise ratio and provides fast acquisition of a large volume. The so-called Indian-ink artifact generates favorable bowel wall visibility. More relevant MRI parameters can be found in the supplementary material, Table S1. During this 10-min 3D cine-MR scan, 160 dynamics were acquired, each consisting of 160 × 160 × 50 voxels, with voxel size of 1.25 × 1.25 × 2.5 mm^3 (Fig. 1, step 1).

2.A.2. Step 2: Deformable image registration

After acquisition of the 3D cine-MRI, the next step was deformable image registration (DIR) of the 160 dynamics. Since bowels rather move in an unpredictable manner than in a periodic manner and no anatomical landmarks could be distinguished on imaging the following approach was chosen: Each consecutive dynamic pair was registered, that is, dynamic two (moving image) was registered onto dynamic one (fixed image). By choosing consecutive dynamics for registration, the time

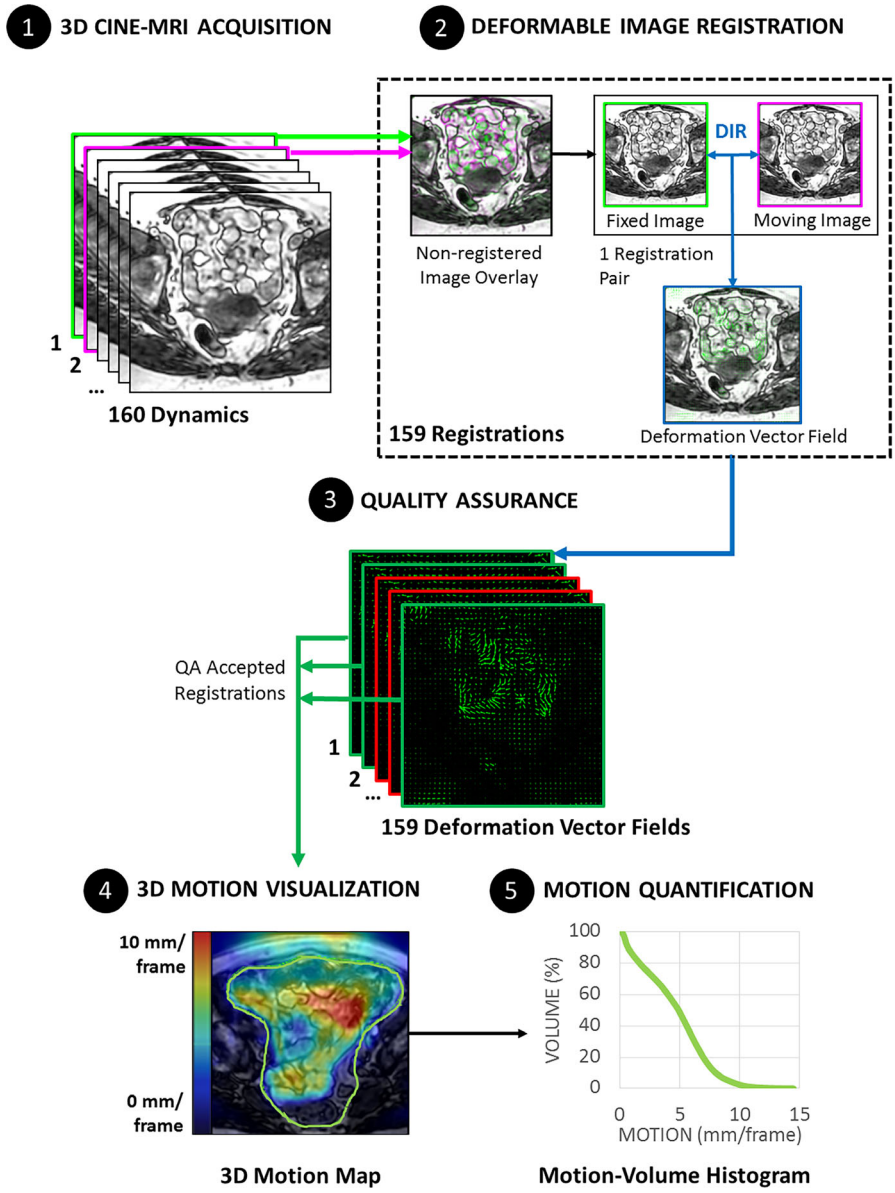

FIG. 1. Schematic representation of the framework for bowel motion visualization and quantification. (1) Per 3D cine-MRI 160 dynamics were obtained. (2) Each dynamic was deformably registered to its preceding dynamic, generating a 3D deformation vector field (DVF), resulting in 159 DVFs per cine-MRI. (3) Quality assurance (QA) was performed for each DVF. (4) From the QA accepted DVFs, the average vector length was calculated per voxel and used to generate a 3D bowel motion map. Finally, the bowel bag volume was manually delineated and (5) a motion–volume histogram (MVH) was obtained. [Color figure can be viewed at wileyonlinelibrary.com]

between time points is minimized which aids the deformable registration quality. This registration procedure was performed for all dynamic pairs of every cine-MRI scan (Fig. 1, step 2).

We applied DIR using a B-spline transformation model as implemented in the Elastix toolbox (version 4.900).[20] In general, a B-spline algorithm optimizes a global similarity measure, such as Mutual Information, and as a result, it presents the deformation field as a parameterized B-Spline.[21] Our applied DIR algorithm used a mutual information image similarity metric and all deformable registrations were performed with a fixed region of interest (ROI) comprising the entire image. The B-spline grid spacing was 2.5 mm, the number of gray level histogram bins was 32, and the number of optimization iterations was 1000. The Elastix configuration file that was used can be found in the supplementary material Section C.

As a result of the DIR, a deformation vector field (DVF) per dynamic pair was generated, describing the magnitude and direction of motion during the time between dynamics (3.7 s). Since the 3D cine-MRI consisted of 160 dynamics, a total of 159 DVFs were generated per MRI acquisition.

2.A.3. Step 3: Quality assurance of deformation vector field generation

The DIR procedure is complex and sensitive to image quality and convergence of the optimization, which might yield errors in the DVFs. Low-quality DVFs in turn may lead

to inaccurate quantification of bowel motion. In order to accurately quantify bowel motion from the DVFs, validation of the applied DIR method was performed, as suggested by the AAPM Task group 132.[22] Since many DIR operations were performed, an automated method was needed for efficient quality assurance (QA). In this study, we determined the Jacobian determinant (JAC) and the Harmonic Energy (HE) for each DVF to investigate whether the DIR transformation was biomechanically and physiologically realistic and gave a numerical robust outcome.[23-25] The DIR QA was applied on the entire DVF and not limited to an ROI since no anatomical landmarks, standard reference nor DVF specific ROI delineation was available.

For each of the 159 DVFs, the Jacobian matrix per voxel was calculated. From this matrix, we derived the JAC[26] and HE[27] per voxel. The JAC describes tissue compression ($0 < JAC < 1$) or expansion ($JAC > 1$). In the literature, the JAC is commonly used for validation of DIR algorithms, since it appears to be a good indicator for the plausibility of a certain transformation.[23,24,26,28] As recommended in these studies, we used in our DIR validation $JAC < 0$, referring to tissue folding, and $JAC > 2$, referring to unrealistic expansion,[22,23] as QA metrics.

The HE is defined as the Frobenius norm of the Jacobian matrix.[27] Concisely the HE is the second derivative of the displacement per voxel in three directions and can be interpreted as a measure of smoothness of the deformable transformation. If DVFs are smooth over all points, the registration can be considered true to nature since all the organ tissue is connected.

Per DVF, the HE on each voxel was calculated from the Jacobian matrix. However, from the literature, a general critical value for the HE was not known. Therefore, a fixed HE value to flag a correct or incorrect registration per voxel was not available as is possible with JAC values.

Finally, in order to summarize quantitatively the quality of each registration in one QA metric, the percentage of voxels with $JAC < 0$ (JAC0%), the percentage of voxels with $JAC > 2$ (JAC2%), and the mean HE (μHE) were calculated over all voxels per DVF. Based on these three QA metrics, all 159 DVFs per MRI were analyzed (Fig. 1, step 4).

Per QA metric (JAC0%, JAC2%, μHE), a cutoff value was determined in order to select the physiologically realistic DVFs and avoid DIR errors influencing motion quantification. If a registration exceeded the cutoff value of one, or more, of these QA metrics, it was sufficient to rule out the DVF. The cutoff value for the QA metrics was population based determined and set at the median + two times the interquartile range (2*IQR) over all registrations of all MRIs.

In order to determine whether the QA metric was indicative for a poor quality registration, both registrations within and outside the cutoff value per QA metric were qualitative evaluated. For this validation, a conventional approach was applied: From the 159 registrations per patient, a selection of DVFs was verified by visually comparing the reference (fixed) image with the deformed floating image. Overlapping the two images allowed to visually perceive the differences between the reference dynamic and deformed dynamic. This was done in VV-viewer (VV: the 4D Slicer, open-source software)[29] using an image fusion tool which merges two images into a single one: The image differences are enhanced with two different colors (green and purple), while the pixel color tends to the original gray levels when differences are low. Perfect DIR should result in a gray image overlay.

2.A.4. Step 4: Three-dimensional motion visualization using a motion map

Per cine-MRI, the set of QA accepted DVFs was used to calculate the vector length per voxel. Subsequently, the average vector length over all included DVFs was calculated. This value is a measure for the average motion magnitude per time frame (3.7 s) at the location of that voxel during the 10-min MRI acquisition. This measure was used to generate a 3D motion map representing the motion per cine-MRI session. The motion map visualizes the location and magnitude of the motion per voxel per time frame on average during the 10-min scan. In the motion map, regions with high average motion (red) and low average motion (blue) can be identified (Fig. 1, step 4).

2.A.5. Step 5: Motion quantification using a motion–volume histogram

In order to further exploit the information conveyed by the DVFs, and to compare motion maps between patients in a quantitative way, we introduce the motion–volume histogram. This concept is similar to the established dose–volume histograms (DVHs) used in radiotherapy. DVHs summarize the simulated radiation dose distribution in a defined ROI[30]: The data are plotted as the volume receiving a dose greater than or equal to a given dose against that dose over the expected dose range. For bowel motion quantification, we have found it useful to plot the data from the motion maps in the same manner. These plots are actually cumulative motion–volume frequency distributions summarizing the entire motion distribution into a single curve for each defined ROI, hereafter refer to them simply as motion–volume histograms (MVHs).

In this study, the bowel bag volume was defined as ROI as follow: The entire peritoneal cavity in which the bowel may be located, inferiorly from the most inferior small bowel loop or above the anorectum, whatever is most inferior, until the most cranial axial slice, and excluding bone, muscle, retroperitoneum, and other organs (such as anal canal, rectum, bladder, and uterus).[31] In the MVH, the motion within the ROI is represented on the x-axis, and the y-axis represents the percentage of volume of the ROI having a motion equal or higher than the x-value (Fig. 2).

Finally, in order to analyze interpatient variation of bowel motion, the following MVH parameters were introduced: M10%, M50%, and M90%. For example, the M50% represents the minimum average bowel motion per frame of 50% of the bowel bag volume.

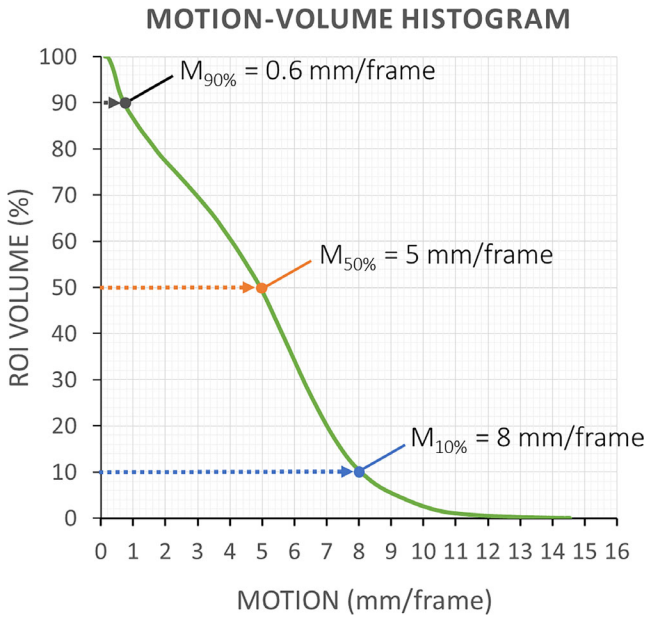

FIG. 2. Example of a motion–volume histogram (MVH) curve and MVH parameter definitions M10%, M50%, and M90%. [Color figure can be viewed at wileyonlinelibrary.com]

2.B. Patient cohort

Patients with gynecological cancer (age >18 yr), treated with curative intent for FIGO stage I-IVA cervical or vaginal cancer or isolated vaginal recurrence of endometrial cancer were included in this study. All patients received external beam radiotherapy (EBRT) to the pelvis, followed by a brachytherapy boost. This study was approved by the medical ethical committee and all patients gave their written informed consent.

2.C. Study protocol

During the MRI session before start of EBRT, the 3D cine-MRI was acquired in addition to the clinical MRI scan protocol. The cine-MR scan was acquired before the administration of the spasmolyticum (Buscopan, Boehringer, Ingelheim, Germany), needed for the clinical protocol. The patients did not receive instruction regarding food and beverage intake before and after the scan sessions.

3. RESULTS

3.A. Deformable image registration validation

Twenty-two datasets of patients were included in this study. Each MRI dataset consisted of among other things 159 registrations. This amounted in 3498 registrations in total, for which DIR QA analysis was performed.

Figure 3 shows the distribution of the three QA metrics over all registrations and the QA values of each registration of each individual patient. Cutoff values were determined at JAC0% = 4.5%, JAC2% = 5.0%, and μHE = 4.0. Patients 6, 9, 20, and 22 had a high incidence of large QA values indicating poorer registration quality. For these patients, more than 10% of the 159 DVFs were rejected. MVH parameters of patient 9 were effected the most by this missing data: A total amount of 147 DVFs were rejected. The poorer registrations in these patients were probably caused by artifacts in the pelvic bones and gas pockets in the bowels. The BTFE sequence is sensitive to magnetic field inhomogeneities and image artifacts due to gas pockets.

Results of DIR and its corresponding HE and JAC maps were qualitatively compared for a subset of the rejected registrations, indicated by the QA metrics JAC0%, JAC2%, and μHE. Figure 4 shows four examples of registrations and the corresponding QA metrics, including two registrations not passing the DIR QA cutoff: Patient 6 (registration 124), JAC0% = 7.1%, JAC2% = 6.2%, μHE = 6.1; Patient 9 (registration 94), JAC0% = 7.1%, JAC2% = 7.3%, μHE = 4.4; and two registrations that pass the DIR QA cutoff: Patient 16 (registration 82), JAC0% = 2.6%, JAC2% = 2.6%, μHE = 3.5; Patient 12 (registration 52) JAC0% = 0.2%, JAC2% = 0.3%, μHE = 3.1.

In the registration examples of both patient 6 and patient 9, not passing the QA cutoff, the image overlay of the reference image and deformed image shows large regions of purple and green coloring, which means the DIR algorithm did not register correctly. In the JAC and HE maps, regions with JAC < 0, JAC > 2, and high HE per voxel (denoted as HE > 4) coincided with regions containing registration errors (i.e., the green–purple mismatches in the images overlay). The DIR errors in patient 6 were mainly outside the bowel bag ROI (where a large error occurred at the abdominal wall), while for patient 9, the DIR errors were also present inside the ROI.

According to the QA measures over all registrations, patient 16 showed higher μHE, JAC0%, and JAC2% errors than patient 12, in which μHE, JAC0%, and JAC2% all were very low. In patient 16, small registration errors exist in the bowel bag volume which might indicate a mismatch and could influence the bowel motion quantification. Moreover, the registrations in patient 12 did not show large regions of green and purple coloring in the image overlay, nor error regions in the JAC and HE maps, confirming the efficacy of the cutoff value. The agreement between the quantitative QA values and qualitative validation confirmed the ability of the QA metrics to detect inaccurate registrations, as shown in Fig. 4.

3.B. Motion visualization using motion maps

From all 22 included study patients, motion maps were generated displaying the average vector length as measure for the average motion per frame in each voxel. The motion map resulted in a clear visualization of areas with small and large movements. Figure 5 shows the motion map of three different patients and the corresponding cumulative MVHs of the bowel bag volume. Patient 11 demonstrated relatively low bowel motion, patient 4 showed medium bowel motion, and patient 16 showed high bowel motion.

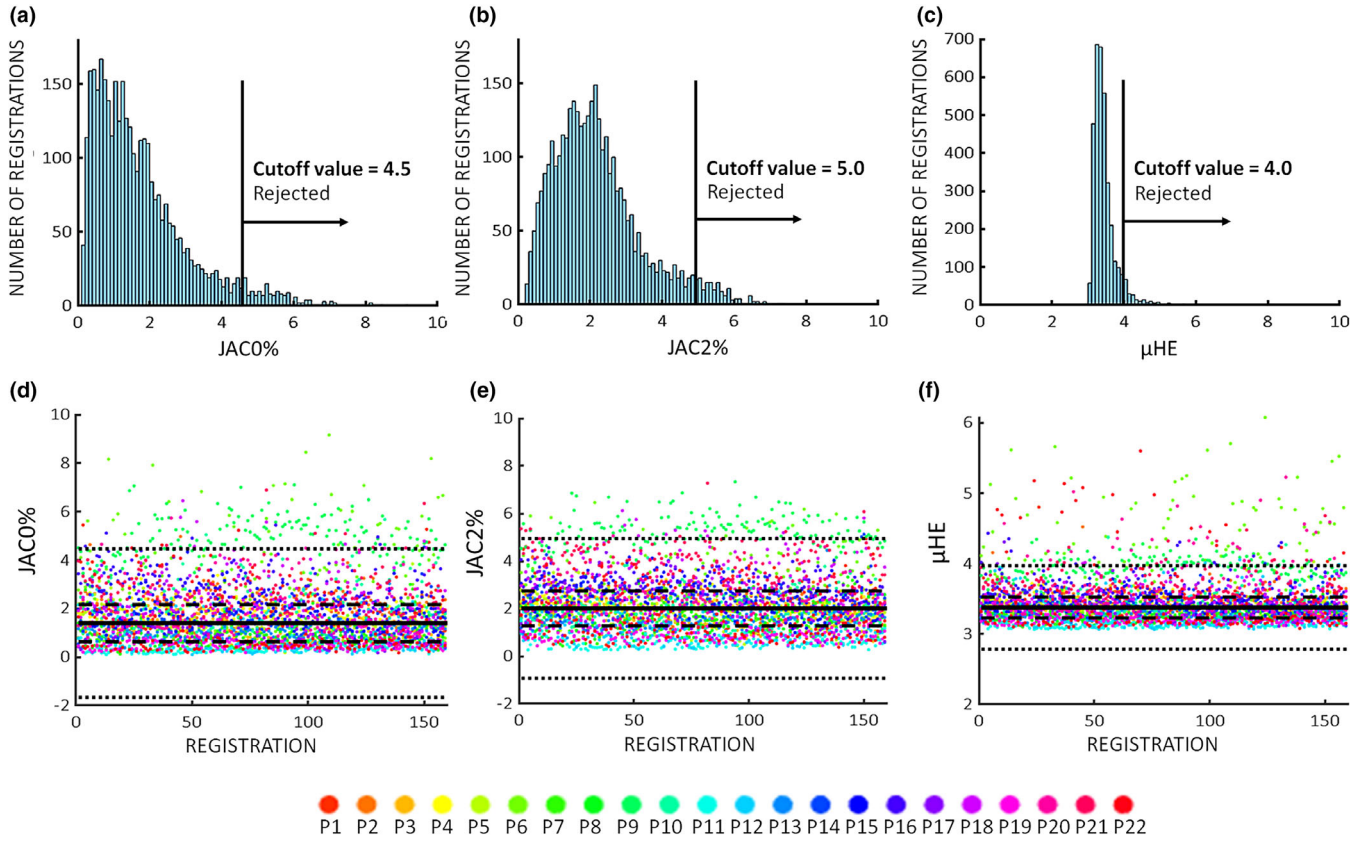

FIG. 3. Distribution of the QA metrics over all registrations of all patients. Top row: Histograms visualizing the distribution of QA metrics for (a) percentage of JAC < 0 (JAC0%), (b) percentage of JAC > 2 (JAC2%), and (c) the mean HE (μHE), over the full patient cohort (3498 registrations). The black lines indicate the calculated cutoff value: median + 2 * IQR point = 4.5, 5.0, and 4.0, respectively. Bottom row: Scatterplots that display (d) the percentage of voxels with JAC < 0, (e) the percentage of voxels with JAC > 2, and (f) the mean HE over all voxels per registration. Every color represents a different patients' MRI, each data point represents one registration. In (d), (e), and (f), the solid black line represents the median of the dataset, median = 1.4, 2.0, and 3.4, respectively. The striped line is the Q1/Q3 of the dataset, with IQR = 1.6, 1.5, and 0.3, respectively. The dotted line represents the cutoff values. Each registration above the cutoff value is considered as a poor quality registration. [Color figure can be viewed at wileyonlinelibrary.com]

3.C. Motion quantification using Motion Volume Histograms

Figure 6 shows the amount of rejected DVFs per cine-MRI and the effect of filtering these DVFs from the MVH data. Figure 7 shows the MVHs determined from QA filtered DVFs for all 22 patients. Interpatient differences in bowel motion are shown, based on the MVHs of the bowel bag and the calculated MVH parameters for all patients. The M10% is 4.4 (range 2.2–7.6) mm per frame on average over all patients. The median average bowel motion, M50%, representing the minimal displacement per frame of 50% of the bowel bag volume with the largest displacement, is on average 2.2 (range 0.9–4.1) mm. The mean M90% is 0.5 (range 0.2–1.4) mm. Since in patients 6, 9, 20, and 22, more than 10% of DVFs were rejected, these MVHs data should be interpreted with caution. Excluding the data of patients 6, 9, 20, and 22, results in a mean M10%/M50%/M90% of 4.4 (range 2.2–7.6) mm/2.1 (range 1.0–4.1) mm/0.5 (range 0.3–1.4) mm.

As shown from the motion maps and MVHs, the variability of bowel motion was high between patients.

4. DISCUSSION

In this study, we demonstrated a technique to visualize and quantify bowel motion in 3D using cine-MRI. The introduction of motion maps and MVHs for the purpose of bowel quantification demonstrates a promising tool for both bowel motion assessment of individual patients and comparison of interpatient bowel motion variability. Finally, the implemented QA metrics, JAC, and HE, and subsequent automatic evaluation of DVFs made the motion map and MVH data less prone to registration errors.

A 3D motion map can pinpoint low motion and high motion regions in the bowel bag of an individual patient. Furthermore, the MVH data comparison shows interpatient variation of 0.9–4.1 mm for the median bowel motion (M50%) and 2.2–7.6 mm for the minimum average bowel motion per frame in a smaller volume of the bowel bag (M10%). Whether this interpatient difference is the result of not giving eating instructions or due to underlying risk factors was beyond the scope of this study. Above all it demonstrates the level of precision at what extend the presented technique enables quantification of bowel motion.

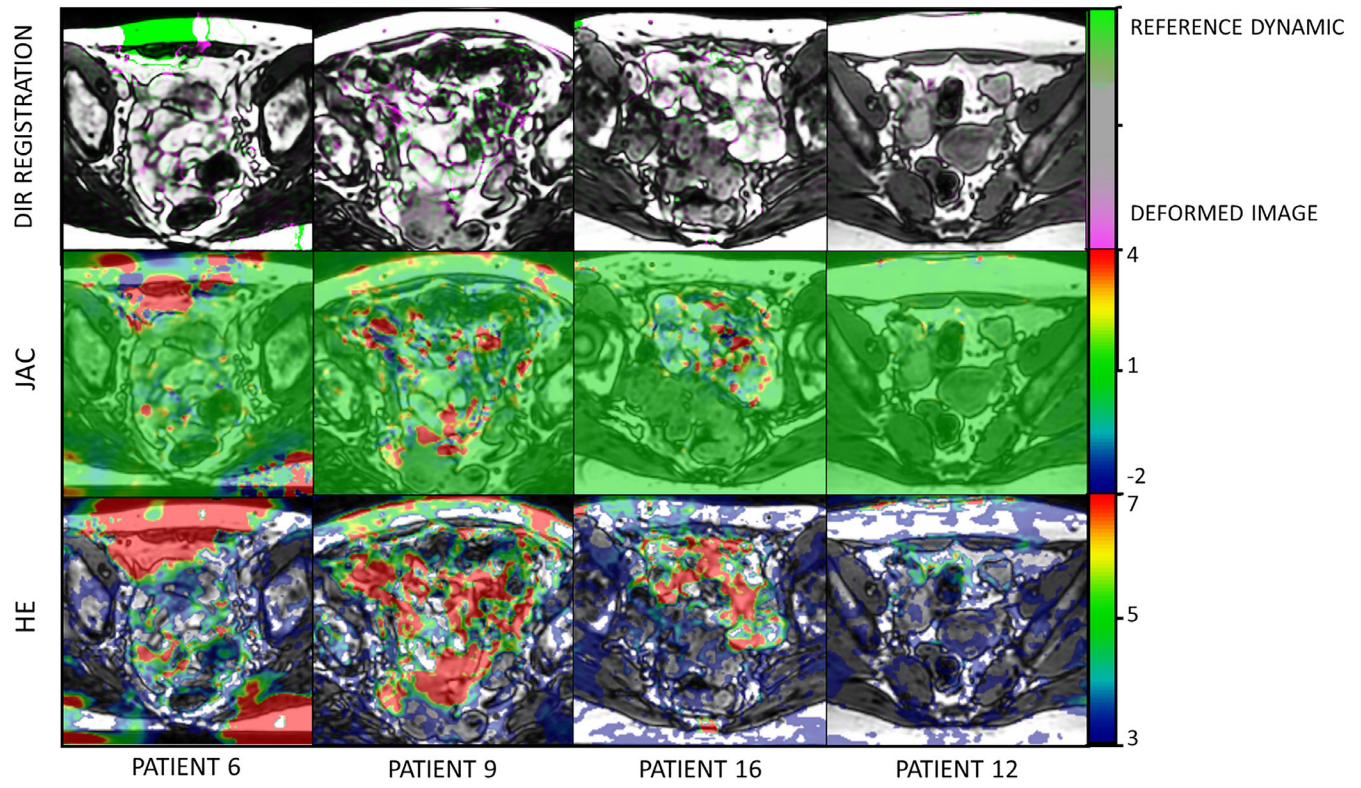

FIG. 4. Examples of deformable image registration (DIR) of one consecutive dynamic pair and the corresponding Jacobian Determinant (JAC) and Harmonic Energy (HE) maps (JAC/HE values per voxel) for four different patients. Top row images show the overlay image of the reference dynamic and deformed dynamic, green and purple indicate incorrect registration. The middle row shows the JAC map, where JAC ranges from −2 to 0 (dark blue to light blue) and JAC ranges from 2 to 4 (yellow to red). Voxels with $0 \leq JAC \leq 1$ (compression) and $1 \leq JAC \leq 2$ (expansion) are colored green. The bottom row shows the HE map, where HE > 4 (turquoise to red) indicates voxels not passing the cutoff value. [Color figure can be viewed at wileyonlinelibrary.com]

The use of the average vector length as motion metric and the MVH as a tool to summarize all 159 vector fields sacrifices directional and spatial information of the motion. This in favor of summarizing the magnitude of motion in the motion maps. The directionality of the motion is present in the DVFs and can always be used for a more detailed analysis per individual patient. However, comparing multiple motion maps is difficult. The MVH concept allows for longitudinal studies, for both comparison between patients and within a patient. Therefore, we emphasize that only the combination of motion map and MVH presents a complete overview in each individual patient.

As a consequence of the applied registration method, registration of consecutive dynamics, the bowel motion maps should be interpreted with care: The motion maps show a surrogate of the bowel wall displacement, namely the amount of displacement per voxel.

The use of motion maps to identify areas of high and low bowel motion is a potential benefit for optimizing radiotherapy treatment plans in the abdominal region. Laan et. al pointed out that gynecological patients with prior major abdominal surgery have a higher risk for severe radiation induced bowel toxicity.[14] One can hypothesize that bowel adhesions result in bowel segments to be fixed in high dose regions where as irradiation of mobile parts of the bowel causes the effective delivered dose to be spread out. The motion map might identify these sparsely moving bowel parts.[32] Sparing of low motion regions during radiotherapy needs to be further investigated since it might be an approach to reduce radiation-induced bowel toxicity.

Important for the reliability of the motion map and MVH data is the accuracy of the applied DIR algorithm. Therefore, quality assurance was performed according to AAPM TG-132 recommendations.[22] According to the literature, it was found that the JAC < 0 and JAC > 2 metrics have proven to be effective for validation of DIR algorithms.[23,24,26,28] Also, one study stated that the HE from B-spline registrations was consistently lower on all their cases compared to other DIR algorithms, indicating that the DVF from B-spline was smoother, and abnormal large values for HE may indicate problems with DVF.[24] Other studies concluded that the HE metric could be used for DIR evaluation in head & neck and lung patients and, moreover, they demonstrate that HE was most accurate.[23] However, a general critical value for the HE was not known in literature. We chose to determine a critical value from population statistics based on 3498 registrations and defined outliers as median+2*IQR. Our results showed that the JAC0%, JAC2%, and μHE QA metrics were able to predict errors in registrations, which is consistent with literature. Our results suggest that both the JAC and HE could be used for DIR evaluation in patients scanned with a 3D cine-MRI acquisition.

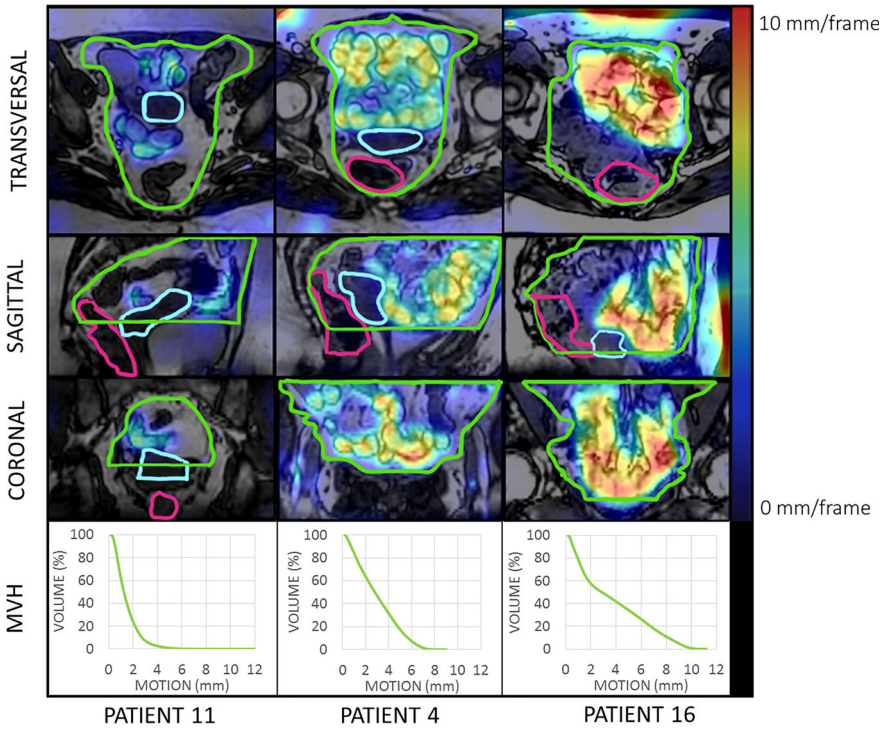

FIG. 5. An example of three patients of the bowel motion maps and its corresponding motion–volume histogram (MVH) of the bowel bag volume (green delineation) excluding the uterus (turquoise delineation) and rectum (pink delineation) volumes. Bowel motion is defined as the mean motion per frame (3.7 s) over the 10-min acquisition, superimposed on an MRI. Red denotes high motion up to 10 mm per frame and blue denotes low motion: the more red the motion map colors, the more mobile was the bowel at that point. [Color figure can be viewed at wileyonlinelibrary.com]

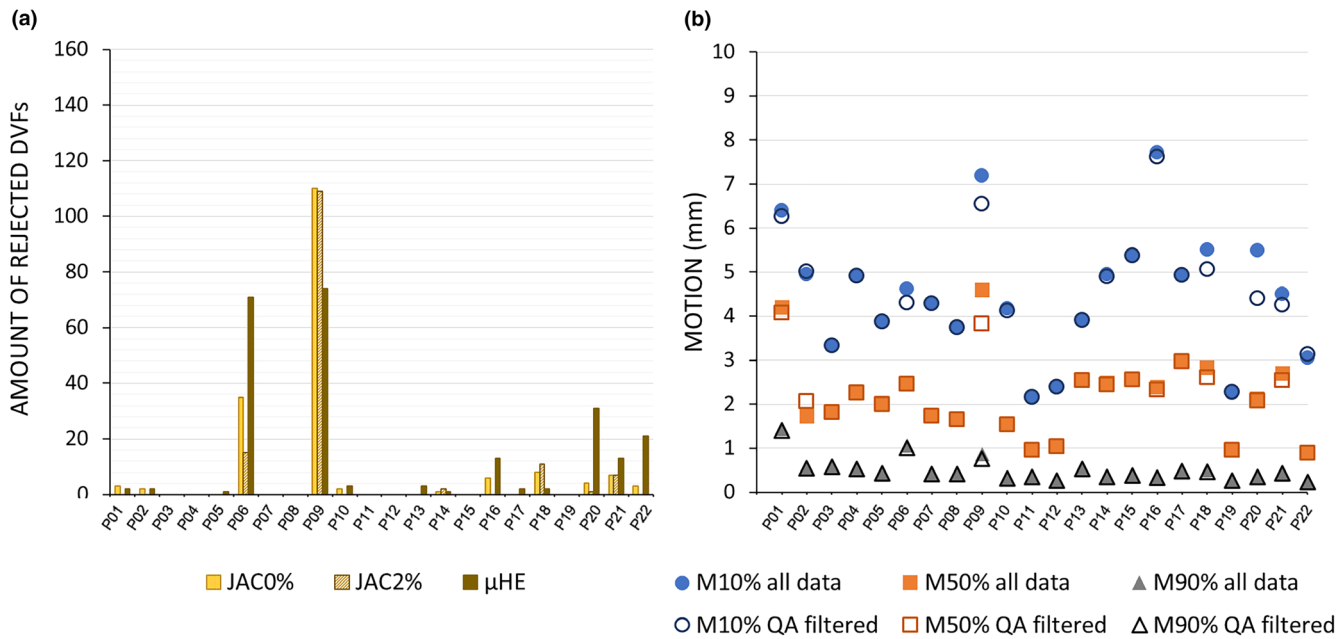

FIG. 6. The results of deformable image registration validation and effect on motion–volume histogram (MVH) parameters. (a) The amount of rejected deformation vector fields (DVFs) based on quality assurance (QA) metrics per patient. (b) The effect of filtering the rejected DVFs from MVH data on MVH parameters M10%, M50%, and M90%. [Color figure can be viewed at wileyonlinelibrary.com]

By visual inspection, it was demonstrated that the QA cut-off values do indeed discriminate between poor and good quality DVFs. However, due to the large amount of data, only randomly sampled visual validation was performed. Additionally, DVFs rejected by one or more of the QA metrics might not be used to generate the motion map and MVH, since these DVFs might be not robust or resulted in an under- or overestimation of bowel motion. Our results indicate that

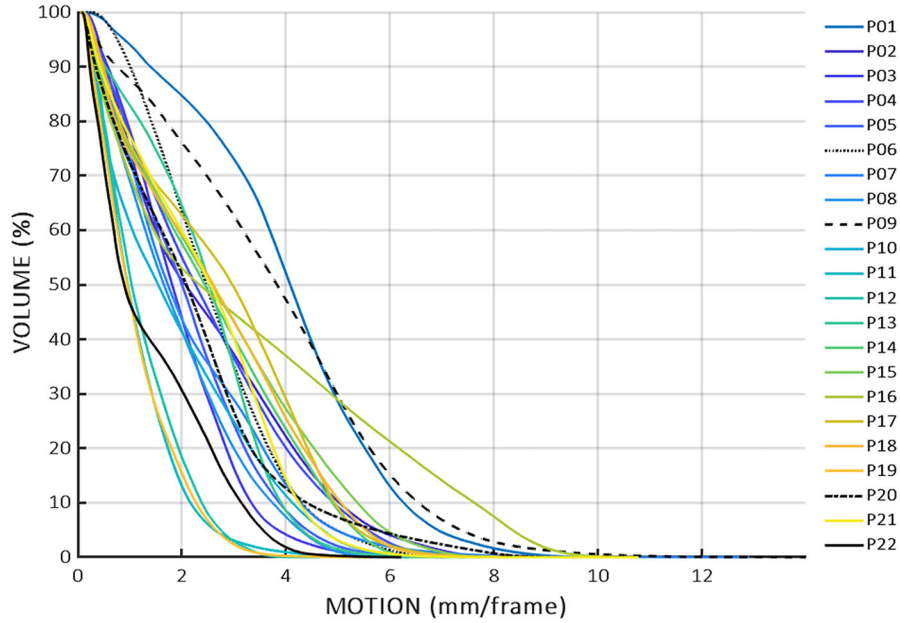

FIG. 7. Motion volume histograms of the bowel bag volume for all 22 patients, based on the average vector length of the QA filtered DVFs. Black lines represent patients 6, 9, 20, and 22 for which more than 10% of DVFs were rejected, which made the MVHs less accurate. [Color figure can be viewed at wileyonlinelibrary.com]

the M10% is most sensitive for filtering poor quality DVFs, which logically follows from the fact that the M10% consists of the largest vector lengths which might be correlated to larger JAC2% and/or HE values. In addition, our results suggest that the impact of small registration errors in the bowel bag ROI on the bowel motion quantification is low, that is, the difference between motion maps and MVH parameters in patient 6 compared to patient 16. However, further validation is necessary at this point.

In this study, a 10-min 3D cine-MR scan was acquired, resulting in the ability to determine intra- and interpatient differences in bowel motion. However, it has not been determined whether 10 min is optimal nor how robust these variables were. It might be that for an accurate and reliable motion quantification shorter or longer timespans are needed. The optimal scan duration (i.e., acquiring more or less dynamics) needs to be assessed and reproducibility must be investigated. Also the consistency and accuracy of the used DIR method need to be further verified. Our current QA method focused on biomechanical and physiological feasibility of registrations. According to the literature, the Inverse Consistency Error and Distance Discordance Metric are suitable metrics to determine DIR accuracy. Implementing one of these QA metrics should be the next step in validation of the accuracy of our DIR technique.[23,24,33,34]

Visual inspection of the dynamic MRI (example in Supplemental Materials, Fig. S1) shows that the bowel motion is captured. Starting from the existing 3D acquisition, speed can be further optimized by deploying acceleration techniques such as compressed sensing.[35,36] This allows to reduce the amount of acquired data points drastically without perceptible loss of information, hence allowing for higher temporal and/or spatial resolution of the 3D cine-MR scan, or scanning at larger field of view. This might enable more precise bowel motion quantification or more advanced analysis techniques such as power spectrum analysis.[8] Also, adding MRI tagging during acquisition[37] may greatly improve the quality of motion quantification as this guides deformable registration algorithms.

We explored the average vector length of DVFs as a measure for bowel motion. However, the average movement can be unnecessarily affected by outliers due to DVFs errors. Furthermore, this metric might be less sensitive to pinpoint the fast large motions or low motion areas. In addition, there is still the need to locate low motion bowel regions, since these regions might correlate to a higher risk of bowel toxicity risk factors, such as adhesions due to abdominal surgery.[14] Therefore, further research is needed to determine other quantification measures, such as the median vector length, maximum vector length, and/or maximum displacement per voxel. If we are able to identify these low or high moving regions, we could incorporate this into our treatment planning and hopefully enable us to better predict dose–effect relationships for the bowel.

5. CONCLUSION

We have developed and validated a novel method to visualize and quantify bowel motion and demonstrated its applicability in a cohort of gynecological cancer patients. In addition, we introduced the concept of motion–volume histograms, which seems to be a promising tool to quantify bowel motion. The median average bowel motion ranges from 0.9 to 4.1 mm per frame (3.7 s) over all patients. This 3D cine-MRI-based quantification tool can be used in further studies to evaluate the clinical relevance of bowel motion

during radiotherapy and has great potential for 3D bowel motion assessment in diagnostic radiology.

CONFLICT OF INTEREST

Potential conflicts of interest: Dr. van Kesteren has involvement in one Varian and one Philips project. Dr. Bel has involvement in several Elekta and Varian sponsored projects. Prof. Stoker and Dr. de Jonge have research collaboration with Takeda and with Motilent concerning MRI of motility. These companies had no involvement in study design, data collection and analysis, or writing of the manuscript. We disclose any and all potential conflicts of interest that could bias the results reported in this work.

DATA AVAILABILITY STATEMENT

The data that support the findings of this study are available from the corresponding author upon reasonable request. The data are not publicly available due to privacy or ethical restrictions.

[a)]Author to whom correspondence should be addressed. Electronic mail: d.l.j.barten@amsterdamumc.nl; Telephone: +31 20 7327826.

REFERENCES

1. Froehlich JM, Patak MA, Von Weymarn C, Juli CF, Zollikofer CL, Wentz KU. Small bowel motility assessment with magnetic resonance imaging. *J Magn Reson Imaging*. 2005;21:370–375.
2. Bickelhaupt S, Froehlich JM, Cattin R, et al. Software-assisted small bowel motility analysis using free-breathing MRI: Feasibility study. *J Magn Reson Imaging*. 2014;39:17–23.
3. Hahnemann ML, Nensa F, Kinner S, et al. Quantitative assessment of small bowel motility in patients with Crohn's disease using dynamic MRI. *Neurogastroenterol Motil*. 2015;27:841–848.
4. Wakamiya M, Furukawa A, Kanasaki S, Murata K. Assessment of small bowel motility function with cine-MRI using balanced steady-state free precession sequence. *J Magn Reson Imaging*. 2011;33:1235–1240.
5. Ohkubo H, Kessoku T, Fuyuki A, et al. Assessment of small bowel motility in patients with chronic intestinal pseudo-obstruction using cine-MRI. *Am J Gastroenterol*. 2013;108:1130–1139.
6. Heye T, Stein D, Antolovic D, Dueck M, Kauczor HU, Hosch W. Evaluation of bowel peristalsis by dynamic cine MRI: Detection of relevant functional disturbances-initial experience. *J Magn Reson Imaging*. 2012;35:859–867.
7. de Jonge CS, Gollifer RM, Nederveen AJ, et al. Dynamic MRI for bowel motility imaging–how fast and how long? *Br J Radiol*. 2018;20170845.
8. Sprengers AMJ, Van Der Paardt MP, Zijta FM, et al. Use of continuously MR tagged imaging for automated motion assessment in the abdomen: A feasibility study. *J Magn Reson Imaging*. 2012;36:492–497.
9. de Jonge CS, Smout AJPM, Nederveen AJ, Stoker J. Evaluation of gastrointestinal motility with MRI: Advances, challenges and opportunities. *Neurogastroenterol Motil*. 2018;30:1–7.
10. Gandhi AK, Sharma DN, Rath GK, et al. Early clinical outcomes and toxicity of intensity modulated versus conventional pelvic radiation therapy for locally advanced cervix carcinoma: A prospective randomized study. *Int J Radiat Oncol Biol Phys*. 2013;87:542–548.
11. Hafiz A, Abbasi AN, Ali N, Khan KA, Qureshi BM. Frequency and severity of acute toxicity of pelvic radiotherapy for gynecological cancer. *J Coll Physicians Surg Pakistan*. 2015;25:802–806.
12. Pötter R, Tanderup K, Kirisits C, et al. The EMBRACE II study: The outcome and prospect of two decades of evolution within the GEC-ESTRO GYN working group and the EMBRACE studies. *Clin Transl Radiat Oncol*. 2018;9:48–60.
13. Jensen NBK, Pötter R, Kirchheiner K, et al. Bowel morbidity following radiochemotherapy and image-guided adaptive brachytherapy for cervical cancer: Physician- and patient reported outcome from the EMBRACE study. *Radiother Oncol*. 2018;127:431–439.
14. Laan JJ, van Lonkhuijzen LRCW, van Os RM, et al. Socioeconomic status as an independent risk factor for severe late bowel toxicity after primary radiotherapy for cervical cancer. *Gynecol Oncol*. 2017;147:684–689.
15. Jackson A, Marks LB, Bentzen SM, et al. The lessons of QUANTEC: Recommendations for reporting and gathering data on dose-volume dependencies of treatment outcome. *Int J Radiat Oncol Biol Phys*. 2010;76:155–160.
16. Kavanagh BD, Pan CC, Dawson LA, et al. Radiation dose-volume effects in the stomach and small bowel. *Int J Radiat Oncol Biol Phys*. 2010;76:101–107.
17. Jadon R, Higgins E, Hanna L, Evans M, Coles B, Staffurth J. A systematic review of dose-volume predictors and constraints for late bowel toxicity following pelvic radiotherapy. *Radiat Oncol*. 2019;14:1–14.
18. Hysing LB, Skorpen TN, Alber M, Fjellsbø LB, Helle SI, Muren LP. Influence of organ motion on conformal vs intensity-modulated pelvic radiotherapy for prostate cancer. *Int J Radiat Oncol Biol Phys*. 2008;71:1496–1503.
19. Kvinnsland Y, Muren LP. The impact of organ motion on intestine doses and complication probabilities in radiotherapy of bladder cancer. *Radiother Oncol*. 2005;76:43–47.
20. Klein S, Staring M, Murphy K, Viergever MA, Pluim JPW. Elastix: A toolbox for intensity-based medical image registration. *IEEE Trans Med Imaging*. 2010;29:196–205.
21. Rueckert D, Sonoda LI, Hayes C, Hill DLG, Leach MO, Hawkes D. Nonrigid registration using free-form deformations: Application to breast mr images. *IEEE Trans Med Imaging*. 1999;18:712–721.
22. Brock KK, Mutic S, McNutt TR, Li H, Kessler ML. Use of image registration and fusion algorithms and techniques in radiotherapy: Report of the AAPM Radiation Therapy Committee Task Group. No. 132: Report. *Med Phys*. 2017;44:e43-e76.
23. Kierkels RGJ, Den Otter LA, Korevaar EW, et al. An automated, quantitative, and case-specific evaluation of deformable image registration in computed tomography images. *Phys Med Biol*. 2018;63:aa9dc2.
24. Varadhan R, Karangelis G, Krishnan K, Hui S. A framework for deformable image registration validation in radiotherapy clinical applications. *J Appl Clin Med Phys*. 2013;14:192–213.
25. Vercauteren T, Pennec X, Perchant A, Ayache N. Diffeomorphic demons: efficient non-parametric image registration. *Neuroimage*. 2009;45:S61–S72.
26. Riyahi S, Choi W, Liu CJ, et al. Quantifying local tumor morphological changes with Jacobian map for prediction of pathologic tumor response to chemo-radiotherapy in locally advanced esophageal cancer. *Phys Med Biol*. 2018;63:aacd22.
27. Forsberg D, Andersson M, Knutsson H. Extending Image Registration Using Polynomial Expansion To Diffeomorphic Deformations. 2013;4–7. https://www.diva-portal.org/smash/get/diva2:509204/FULLTEXT01.pdf.
28. Fatyga M, Dogan N, Weiss E, et al. A voxel-by-voxel comparison of deformable vector fields obtained by three deformable image registration algorithms applied to 4DCT lung studies. *Front Oncol*. 2015;5:1–9.
29. Seroul P, Sarrut D. VV: A viewer for the evaluation of 4D image registration. *Midas J*. 2008;1–8. http://hdl.handle.net/10380/1458.
30. Drzymala RE, Mohan R, Brewster L, et al. Dose-volume histograms. *Int J Radiat Oncol Biol Phys*. 1991;21:71–78.
31. Gay HA, Barthold HJ, O'Meara E, et al. Pelvic normal tissue contouring guidelines for radiation therapy: A radiation therapy oncology group consensus panel atlas. *Int J Radiat Oncol Biol Phys*. 2012;83.
32. Yasemin A, Mehmet B, Omer A. Assessment of the diagnostic efficacy of abdominal ultrasonography and cine magnetic resonance imaging in detecting abdominal adhesions: A double-blind research study. *Eur J Radiol*. 2020;126:1–6.
33. Bender ET, Tomé WA. The utilization of consistency metrics for error analysis in deformable image registration. *Phys Med Biol*. 2009;54:5561–5577.
34. Saleh ZH, Apte AP, Sharp GC, et al. The distance discordance metric - A novel approach to quantifying spatial uncertainties in intra- and inter-patient deformable image registration. *Phys Med Biol*. 2014;59:733–746.

35. Lustig M, Donoho D, Pauly JM. Sparse MRI: The application of compressed sensing for rapid MR imaging. *Magn Reson Med*. 2007;58:1182–1195.
36. de Jonge CS, Coolen BF, Peper ES, et al. Evaluation of compressed sensing MRI for accelerated bowel motility imaging. *Eur Radiol Exp*. 2019;3:7.
37. de Jonge CS, Sprengers AMJ, van Rijn KL, Nederveen AJ, Stoker J. Assessment of fasted and fed gastrointestinal contraction frequencies in healthy subjects using continuously tagged MRI. *Neurogastroenterol Motil*. 2020;32:1–8.

SUPPORTING INFORMATION

Additional supporting information may be found online in the Supporting Information section at the end of the article.

Fig. S1. Movie loop of 160 dynamics of patient 4.
Table S1. MRI acquisition parameters for the bowel motion scan.